Appl Phys A (2011) 103:1021–1031
DOI 10.1007/s00339-011-6384-2

Applied Physics A
Materials Science & Processing

Reactive diffusion in Sc/Si multilayer X-ray mirrors with CrB_2 barrier layers

Y.P. Pershyn · E.N. Zubarev · V.V. Kondratenko · V.A. Sevryukova · S.V. Kurbatova

Received: 14 May 2010 / Accepted: 11 February 2011 / Published online: 14 April 2011

Abstract Processes undergoing in Sc/Si multilayer X-ray mirrors (MXMs) with periods of ∼27 nm and barrier layers of $CrB_2$0.3- and 0.7-nm thick within the temperature range of 420–780 K were studied by methods of small-angle X-ray reflectivity ($\lambda = 0.154$ nm) and cross-sectional transmission electron microscopy. All layers with the exception of Sc ones are amorphous. Barrier layers are stable at least up to a temperature of 625 K and double the activation energy of diffusional intermixing at moderate temperatures. Introduction of barriers improves the thermal stability of Sc/Si MXMs at least by 80 degrees. Diffusion of Si atoms through barrier layers into Sc layers with formation of silicides was shown to be the main degradation mechanism of MXMs. A comparison of the stability for Sc/Si MXMs with different barriers published in the literature is conducted. The ways of further improvement of barrier properties are discussed.

1 Introduction

Multilayer X-ray mirrors (MXMs) are efficient reflective elements [1] widely used in the soft X-ray and extreme ultraviolet band ranging from ∼0.3 to almost 70 nm [2, 3]. Consisting of alternating layers of high and low refractive indexes, they can easily take the shape of flat or figured substrates and enhance by many times the reflectivity of multilayered optics compared to single-material optics. The best expected optical performance of the MXMs is defined by the selection of material pairs. That is why such multilayers as a rule constitute a multiphase non-equilibrium system and in consequence tend to degrade sometimes even at small external exposure, for instance warming [4], irradiation [5] or just with time [6, 7]. This circumstance restricts applications of MXMs, so a number of approaches improving MXM stability were proposed [8–11]. One of these approaches is utilization of barrier layers [11, 12] slowing down diffusion intermixing that is one of the main degradation mechanisms during thermal loads. Selecting a barrier material, optimizing its deposition conditions and keeping the MXM reflectivity high are the subject of technological and scientific efforts.

Scandium–silicon (Sc/Si) multilayers were shown to be effective in the wavelength range of 38–50 nm with reflectivities of 30–50% at normal incidence [13]. They demonstrated their feasibility in laser interferometry [14], polarimetry [15], ellipsometry [16], spectroscopy [17] and microscopy with nano-scale resolution [18]. Sc/Si MXMs could focus laser energy ($\lambda = 46.9$ nm) to the intensity of up to $\sim 10^{11}$ W/cm^2 that is in excess of the ablation threshold for metallic materials [19]. However, in spite of successful application of this material pair, Sc/Si MXMs degrade at as low a temperature as 370 K [20, 21] and even less [22]. It was also reported [23] that the damage threshold for Sc/Si MXM during laser irradiation with a wavelength of 46.9 nm is an order of magnitude less than that for bulk silicon. Thus, there is a necessity to improve the stability of the Sc/Si multilayer system. Besides Sc/Si, MXMs have intermixed interlayers at each interface formed during the deposition process [13]. Depending on deposition conditions, the interlayer thickness may attain 3–5 nm [5, 24] that decreases the efficiency of multilayer mirrors noticeably. Decreasing the interlayer thickness will considerably improve their efficiency.

Y.P. Pershyn (✉) · E.N. Zubarev · V.V. Kondratenko · V.A. Sevryukova · S.V. Kurbatova
National Technical University 'Kharkiv Polytechnic Institute', 21 Frunze Street, Kharkiv 31002, Ukraine
e-mail: pershyn@kpi.kharkov.ua
Fax: +38-057-7076601

In this paper the processes taking place in Sc/Si MXMs with CrB_2 barrier layers during thermal annealing are studied. The material CrB_2 was chosen because of its high melting temperature (2473 K), so it is expected that diffusion processes in this system will be shifted to higher temperature compared to the MXMs with Cr barriers [22]. It is also known that chromium does not interact with scandium [25], so a Sc/barrier interface should noticeably decrease the diffusion mobility of scandium. In addition, borides are used as barriers in silicon technology for VLSI fabrication [26, 27]. Therefore, we expect that CrB_2 will prevent diffusion of components during both deposition and annealing.

Different barrier materials have been used for the Sc/Si system [20–22] but these studies are mainly focused on the stability of optical properties. We consider structural changes responsible for the degradation of Sc/CrB_2/Si MXMs to ascertain their hierarchy and to establish the ways of further improvement of MXM stability.

2 Experiment

Sc/CrB_2/Si MXMs were fabricated by the method of DC magnetron sputtering. Three targets (Si, CrB_2 and Sc) ∼100 mm in diameter and with a purity of better than 99% were used for layer deposition. Multilayer coating was applied by successive movement of a substrate over each of three magnetrons. Since three magnetron sources of matter were available in the vacuum chamber and each MXM period contained four layers (a barrier layer at every interface), the substrate holder executed a pendulum motion passing over the CrB_2 target twice. Deposition rates were kept constant and were ∼0.24 nm/s for Sc, ∼0.13 nm/s for CrB_2 and ∼0.38 nm/s for Si. The nominal fraction of the high-absorbing (Sc + CrB_2) layer in the period was ∼0.4. The average composition of the MXMs excepting barrier layers was close to $ScSi_{1.9}$. It means that after full reaction between Sc and Si with formation of Sc_3Si_5 silicide [24], a small Si interlayer should remain but Sc is consumed entirely.

Argon pressure in the vacuum chamber during the deposition run was ∼0.4 Pa. Before a deposition process the vacuum chamber was baked to degas internal equipment. Both silicon wafers and float glass with RMS roughness of 0.3–0.5 nm were used as substrates.

Annealing of deposited samples was made in another vacuum chamber at the pressure of residual gas atmosphere of less than 4×10^{-4} Pa. Samples with minimum dimensions of $\sim 10 \times 20$ mm^2 were heated by infrared lamps in a stainless steel envelope and its temperature was controlled by a calibrated chromel–alumel thermocouple. Utilization of such construction gave a possibility for the gradient over the sample surface to be extremely low. The annealing temperature was stabilized by a high-precision temperature-control device (RIF-101, Russia) with a precision better than ±1°. The range of annealing temperatures was 420–780 K. Up to ∼600 K samples were annealed with a step of ∼50° and at higher temperatures the step was ∼25°. The annealing time at each temperature amounted to 1 h.

Each prepared and annealed sample was measured in a small-angle geometry at an X-ray diffractometer (DRON-3M, Russia) assembled as a double-crystal spectrometer with a (110)Si primary-crystal monochromator. The monochromator in combination with a 0.1-mm slit allowed us to select only a characteristic line of copper Cu$K\alpha_1$(0.154059 nm) from the hard X-ray spectrum. The beam divergence was ∼0.015°. Taking into account the measurement range for angles, we could control a MXM period with a precision better than 0.01 nm. Phase analysis of annealed samples was performed at another X-ray diffractometer supplied with a (002) graphite analyzer selecting the Cu$K\alpha$ line.

To directly observe the process of changing the geometrical construction of Sc/CrB_2/Si MXMs and a structure of individual layers after annealing, cross sections of some samples were studied in a transmission electron microscope (TEM, PEM-U, Ukraine) having line resolution (atomic planes) of ∼0.2 nm. All scales in TEM images were calibrated with X-ray measurements. The procedures of cross-section preparation are described earlier [28, 29].

3 Results

3.1 Characterization of as-deposited state

We prepared several identical Sc/Si multilayers with CrB_2 barriers at each interface. Most of them have periods close to 27 nm. That corresponds to the reflection of soft X-rays with a wavelength of ∼47 nm at normal incidence. Nominal thicknesses of barriers at adjacent interfaces differed and amounted to ∼0.3 nm (Sc-on-Si interfaces) and ∼0.7 nm (Si-on-Sc interfaces). The reason for this difference consists in the following. During reflection at Bragg angle a standing wave forms within a MXM volume with nodes being at Si-on-Sc interfaces and antinodes being in the vicinity of Sc-on-Si interfaces [30]. Since, compared to Sc and Si, chromium diboride is a more absorbing material, to retain high multilayer reflectivity we should make a barrier layer as thin as possible at the interfaces with high amplitude of electromagnetic field (Sc-on-Si ones). We deposited CrB_2 layers ∼0.3-nm thick at these interfaces to be the low limit wherein the barrier layer separates Sc from Si layers. At the adjacent interfaces the thickness of the barrier layer is not so critical.

Characterization of multilayers was made by processing low-angle ($2\theta < 8°$) X-ray diffraction curves. One of

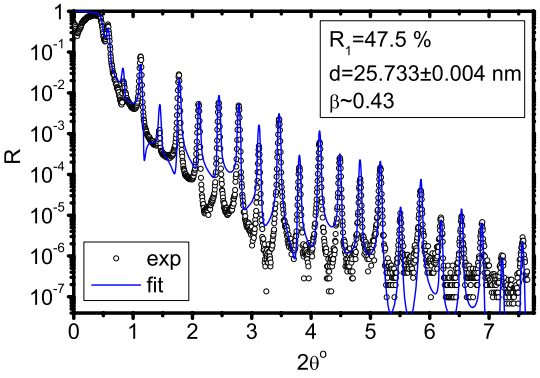

Fig. 1 Small-angle diffraction pattern for Sc/CrB_2/Si/30 MXM on a float glass substrate measured in hard X-ray region at $\lambda = 0.154059$ nm (*dotted curve*) and fit (*solid curve*)

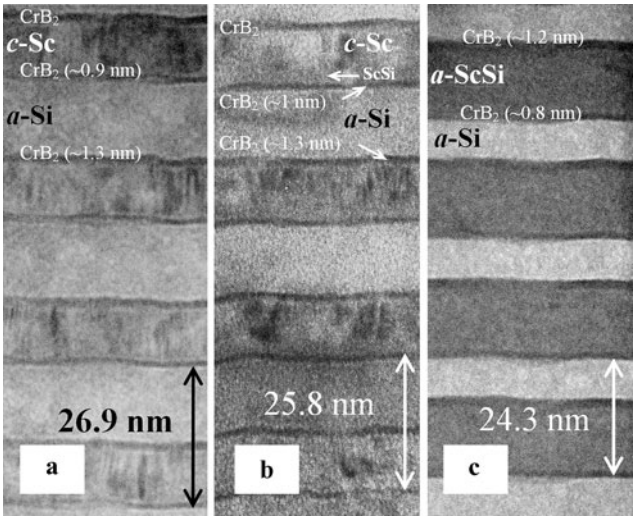

Fig. 2 Cross-sectional TEM images of Sc/CrB_2/Si MXMs in as-deposited state (**a**) and after annealings at $T = 525$ K (**b**) and $T = 625$ K (**c**) for 1 h

such curves for a 30-period MXM on a float glass substrate is shown in Fig. 1 as small circles. More than 20 diffraction peaks are visible in it, indicating a good periodicity for the measured multilayer. Weak suppression of 2nd and 4th diffraction peaks suggests that the fraction, β, of the high-absorbing layer (Sc + CrB_2) in the period is close to 0.5. Though the nominal fraction is $\beta \sim 0.4$, the theoretical curve (solid line) with this parameter does not fit the experimental one quite well. Best fit was achieved at $\beta \sim 0.43$ and mean interface roughness $\sigma \sim 0.48$ nm but we did not manage to reasonably suppress 2nd and 4th peaks even for fractions ranging from 0.4 to 0.6 and the same roughness for all interfaces. In the case of the X-ray diffraction curve given in Fig. 1, the period (d_0) was measured to be 25.73 ± 0.01 nm.

Reflecting curves for MXMs on Si substrates had reflectivities 10–70% less than those on float glass ones especially at angles $2\theta < 2°$. The reason for that is a small bend of thin (~0.4 mm) silicon substrates that brings about the reflectivity underrating. Therefore, to estimate an interface roughness, σ, we used an empirical formula (see Appendix) and obtained that on average the interface roughness of Sc/CrB_2/Si MXMs deposited onto Si substrates does not exceed 0.67 nm. In spite of bending of the substrates, the angle positions of peaks are little affected, so the MXM periods were determined from the angle positions of diffraction peaks taking into account refraction.

A cross-sectional image of a Sc/CrB_2/Si MXM on a Si substrate is shown in Fig. 2a. By the electron diffraction pattern (not shown) and the presence of image diffraction contrast we concluded that Sc layers were crystalline and Si and barrier layers were amorphous. Crystalline scandium occupies the space between two barrier layers. The fraction of high-absorbing layer is ~0.46, exceeding the nominal one (see Sect. 2). The barrier layers have increased thicknesses to be ~0.9 nm (Sc-on-Si interfaces) and ~1.3 nm (Si-on-Sc interfaces). That is about 0.6-nm thicker than nominal values, indicating some interaction between barrier layers and Sc and/or Si. This interaction is the cause of increasing β. Having compared nominal and experimental thicknesses of barrier layers, we deduced that a 0.7-nm barrier (Si-on-Sc interface) interacted with the parent materials only partially. The same difference between nominal and experimental values of layer thicknesses is evidence that a sublayer of ~0.4 nm within the thick barrier layer could be compositionally identical to CrB_2. The scandium thickness measured in the TEM image is ~10 nm that is in agreement with the nominally deposited value. It denotes that barrier layers react mainly with silicon.

It is worth noting here that barrier thickness is considerably less than the thickness of interlayers in Sc/Si MXMs even subject to the broadening. So, CrB_2 can be used at least at a Sc-on-Si interface where the interlayer thickness is a critical parameter affecting MXM efficiency [22, 30].

3.2 Annealing of MXMs

3.2.1 Hard X-ray study

To study the MXM behavior at elevated temperatures, two identical Sc/CrB_2/Si samples were fabricated with a periodicity of ~27 nm. Such number of samples, on one hand, enables us to improve reliability of received data and, on the other hand, to reasonably restrict the volume of research efforts. Since float glass begins softening at temperatures of $T > 670$ K, only MXMs on Si substrates were subjected to the heat treatment.

The overall picture of small-angle diffraction curve behaviors for annealed samples shows that with a rise of temperature the number of diffraction peaks is reduced (from 20 in as-deposited state down to 6 at 780 K) and integral curve

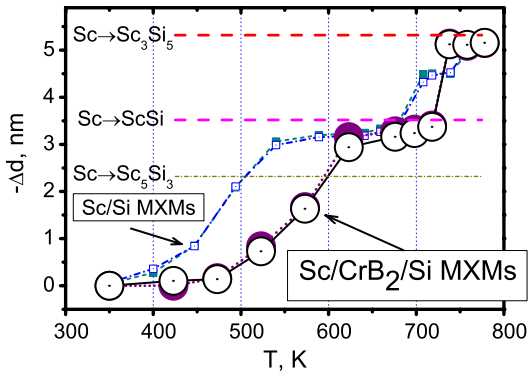

Fig. 3 Period contraction, Δd (*circles*), versus annealing temperature for two Sc/CrB_2/Si MXMs. Similar data for Sc/Si MXMs are designated by *small squares*

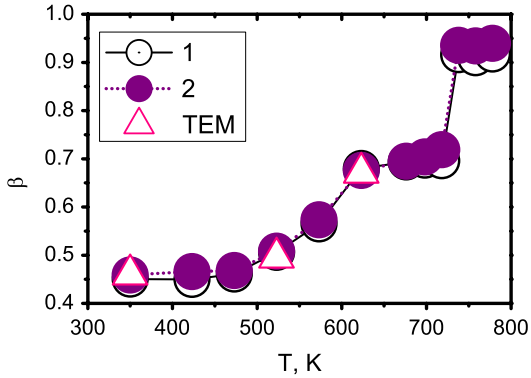

Fig. 4 Estimated values for fractions, β (*circles*), of the high-absorbing layer (Sc + CrB_2) in the period of Sc/CrB_2/Si MXMs depending on annealing temperature. Experimental values of β taken from TEM images are designated by *triangles*

intensities diminish that may suggest interface roughening and component intermixing. Diffraction peaks were shifted toward large angles that indicates a period contraction in the multilayer systems.

As was found earlier [24], diffusion intermixing with the formation of silicides and respective volume shrinkage are characteristic for heated Sc/Si MXMs. We also associated the volume change in Sc/CrB_2/Si MXMs with the phase formation and involved the period contraction as a measure of diffusion intermixing. A graph of the period contraction, Δd ($= d - d_0$, with d_0 being the as-deposited period), as a function of annealing temperature for both samples is shown in Fig. 3 and designated by circles. The first experimental point for each sample corresponds to the initial state. Since the substrate may be heated at maximum up to ~350 K during the process of deposition, we have taken it as the initial substrate temperature. The observed small distinction in contractions of the samples is most likely connected with small-scale difference in thickness, structure and/or composition of barrier layers.

The highest possible contraction connected with interaction of a barrier layer ~1-nm thick with the parent materials was estimated to be less than 1 nm. That is well below the observed range of experimental contractions reaching up to ~5 nm (Fig. 3). Besides, as was revealed in the TEM study, the barrier material is almost half reacted in the as-deposited state (see Sect. 3.1). So, we accepted that on heating Sc layers interact mainly with Si ones and neglected the possible contraction relating to interaction of barrier layers.

At the beginning of heating the amorphous ScSi monosilicide is incipient in pure Sc/Si and Sc/W/Si MXMs that is observed for a variety of period values and layer thicknesses [20, 24, 31, 32] and thereupon ScSi may crystallize for thick ($t > 50$ nm) layers [33] or transform into amorphous Sc_3Si_5 [24, 31]. Since in our case layer thicknesses do not exceed 16 nm, by analogy we assumed that ScSi silicide formed initially in barrier MXMs at the first stage, and after the consumption of scandium layers ScSi transformed into amorphous Sc_3Si_5 silicide at the second stage. So, now we can try to distinguish the stage of completing ScSi formation and transition to Sc_3Si_5. It is visible in Fig. 3 that after 625 K the run of the curve slow down. As diffusion is a temperature-activated process, this retardation may indicate the onset of Sc_3Si_5 formation taking into consideration a decay in gradient of chemical potential concerned with a drop in concentration gradient.

We also added to Fig. 3 the behavior of Sc/Si MXMs (denoted by small squares) annealed under identical conditions. As may be seen, they behave in a closely parallel manner: ScSi silicide is formed initially ($T < 540$ K), then a slow transition of ScSi into Sc_3Si_5 (540 K $< T <$ 680 K) proceeds and afterward a jump in $|\Delta d|$ at $T > 700$ K completes the similarity. The major distinction for Sc/CrB_2/Si MXMs is some shift of 80–100° upwards on the temperature scale for majority processes taking place in the Sc/Si system. That also refers to the beginning of active ScSi formation and crystallization of Sc_3Si_5 at elevated temperatures.

After such preliminary deduction, we used the contraction values to estimate the thickness of Sc-containing layers and added the experimental barrier thicknesses. Then, having divided the sum by the experimental periods, we defined the expected fractions β. The plot of $\beta(T)$ can be seen in Fig. 4 in the form of light and dark circles. The growth of β from ~0.46 in as-deposited state up to ~0.93 at the end of annealing is seen. Variation in β should be accompanied by an intensity redistribution between diffraction peaks inducing some of them to grow and others to drop. Indeed, after annealing at $T \sim 525$ K, where according to the estimation $\beta \sim 0.51$, we observed a suppression of even maxima including the 12th one in the small-angle diffraction pattern and, at $T \sim 720$ K with $\beta \sim 0.71$ (the value being close to 0.75), the 4th maximum was noticeably suppressed. In other words, there exists a correlation between experiment and formal calculations that indicates the validity of our assumption.

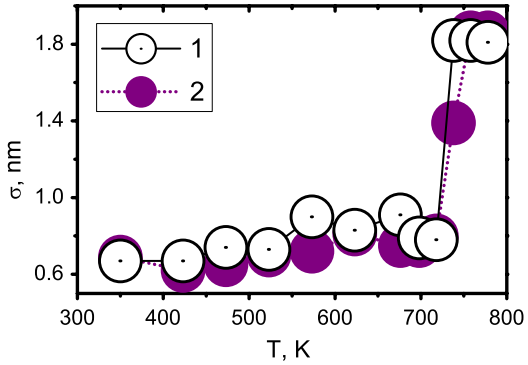

Fig. 5 Evolution of root-mean-square roughness, σ, for interfaces in $Sc/CrB_2/Si$ MXMs with annealing temperature

At temperatures $T > 575$ K when the fraction β exceeds ~0.6, an appreciable drop in $Sc/CrB_2/Si$ MXM reflectivity may be expected. Although this fact takes place with reflectivities decreasing from ~33% to ~4% at temperatures higher than 575 K, we can only qualitatively rely on this fact. The reason for this consists in the growth of the reflectivity from ~16% to ~30% within the range of 350–575 K which should not occur, and we associate that with changing the shape of the Si substrate and its focusing/defocussing ability.

Using the empirical formula for evaluating the interface roughness (see Appendix), we illustrated its evolution in Fig. 5. Multilayer interface roughness, as is visible from the presented data, increases slowly from ~0.7 nm till 0.8–0.9 nm at temperatures $T < 730$ K and jumps up till ~1.8 nm at $T > 730$ K. Such jump denotes abrupt changes in the MXM structure, which are most likely connected with a crystallization of Sc_3Si_5. The experimental fact of Sc_3Si_5 silicide crystallization in Sc/Si MXMs at $T \sim 700$ K observed earlier [31] can be an argument benefiting this idea. In addition, by X-ray phase analysis we observed the presence of Sc_3Si_5 together with $CrSi_2$ and traces of SiB_4 phases in MXMs after a full cycle of the annealing.

For one of the samples annealed at the highest temperature we fitted a modeled small-angle curve to the experimental one using the roughness as an adjustable parameter and considering the high-absorbing layer as Sc_3Si_5 silicide with its fraction as given in Fig. 4. Best fit to the experiment was attained at roughness $\sigma \sim 1.7$ nm that is close to the preliminarily estimated value of ~1.8 nm. Although such roughness is rather large, it comes to only 8% of the MXM period. Using the Debye–Waller factor it can be shown that such roughness decreases the MXM reflectivity by no more than 25%. Since multilayer reflectivity drops several-fold during annealing, we may conclude that the change in the fraction β and not in the roughness exerts the primary control over the MXM reflectivity.

3.2.2 TEM study

Inasmuch as the final stages of damage are of the least interest from the standpoint of possible optical applications, we conducted a TEM study for the samples annealed at temperatures of 525 K and 625 K that approximately corresponded to the beginning and the middle of the MXM degradation process (see Fig. 3). Cross-sectional TEM images of multilayer samples for both temperatures are shown in Fig. 2b and c, correspondingly.

An examination of the sample annealed at $T \sim 525$ K (Fig. 2b) shows that the degradation process is well noticeable: the ratio of layer thicknesses was varied within the period ($t_{Sc}/t_{Si} \approx 0.7 \rightarrow 0.6$; $\beta \approx 0.46 \rightarrow 0.49$); the thickness of crystalline scandium decreased; an amorphous interlayer appeared at the bottom Sc interface as viewed from the thin barrier layer. From the consumption of Sc and Si layers and the period contraction we determined that the composition of the amorphous interlayer ~2.1-nm thick is close to ScSi monosilicide. No signs of Sc and Si interaction at the top Sc interface were revealed. We see that at least a 0.7-nm CrB_2 layer may be suitable as a barrier at this annealing temperature. By a marker method it has been earlier shown that silicon is the fast diffusion species for the Sc/Si multilayer system [32]. In the studied samples the amorphous interlayer grows from one side of the barrier, namely from the side adjacent to scandium (see Fig. 2a). Thus, it may be inferred that in Sc/Si MXMs with barrier layers, silicon is the fast diffusion species, too.

The annealing of the multilayer sample at 625 K results in its total amorphization (Fig. 2c). In the electron diffraction pattern the rings corresponding to crystalline scandium disappeared and a few halos remained instead. So, both the image and the electron diffraction pattern show no signs of pure scandium. The fraction of the high-absorbing layer in the period rises to $\beta \sim 0.67$. The composition of the Sc-based layer estimated from the ratio of layer thicknesses is also close to ScSi monosilicide.

Despite the started diffusion intermixing of Sc and Si layers, barrier thicknesses at both interfaces are fixed at about the same thickness as in the as-deposited state (~0.9 and ~1.3 nm). This suggests that CrB_2 is inert with respect to Sc and Si at least up to 625 K. It is conceivable for the thin barrier layers to be inert to silicon atoms diffusing through, as they already reacted with MXM material in the as-deposited state. However, thicker barriers reacted in the as-deposited state only partially are stable.

The fractions of high-absorbing layers including barrier layers for both annealing temperatures are designated in the form of triangles in Fig. 4. Good agreement is observed with different data even though Fig. 4 was originally plotted based on estimated values.

Relying on bulk densities for Sc, Si and silicides, we evaluated maximum contractions being possible for the studied

MXMs which accompany transitions of Sc into one of three silicides, namely Sc_5Si_3, ScSi and Sc_3Si_5. Results of our estimations were plotted in Fig. 3 as horizontal lines. Using these lines as a support, one may ascertain again that there is no feature concerned with the formation of Sc_5Si_3 silicide and diffusional intermixing occurs with participation of ScSi and Sc_3Si_5 only. It is also visible that supporting lines for the latter silicides are above the respective experimental points being considered as the stages of ScSi and Sc_3Si_5 appearance, although the reaction of barrier layers was disregarded here. This disagreement is too large to be explained by the inaccuracy of the experiment measurements. Lower experimental values for Sc/Si MXMs are understood if the presence of interlayers is allowed. However, this is not the case for Sc/CrB_2/Si MXMs. We see the following reasons explaining this contradiction. It is known that thin films can have lower density compared to the bulk [34–37]. In particular, scandium and silicon layers were reported to have reduced density by 6–10% [38]. Since experimental volume ratios of reacted components are characteristic for the corresponding bulk silicide, and component layers have reduced densities, silicides formed during annealing cycles may also have reduced densities. Direct comparison of the experimental data with estimations gives at least 10% reduction of the density for ScSi and 3–4% for Sc_3Si_5, though taking into account possible interaction of barrier layers at high temperature the latter values can be less. In addition, although experimental volume ratios of consumed Sc and Si layers at moderate temperatures are close to that for ScSi silicide, they always yielded an excess of Sc exceeding the nominal value by 3–10%. So, in spite of the existence of precise stoichiometry for ScSi silicide in the equilibrium phase diagram, we suppose that the formation of compounds with a wide homogeneity region in the amorphous state is possible as was considered earlier [39, 40]. We expect that in the Sc/CrB_2/Si system the amorphous compounds of $ScSi_{1-x}$ and Sc_3Si_{5-x} may be formed. Now taking into account lower densities for component layers and the silicides and the potential non-stoichiometry, it is clear that bulk Sc density used in calculations of the reference lines should give the overestimated values.

3.3 Evaluation of diffusion characteristics

Diffusion intermixing in Sc/CrB_2/Si MXMs is attended with the formation of new phases, i.e. reactive diffusion occurs. Thus, we can evaluate diffusivities by the following formula [41, 42]:

$$D = \frac{x^2 - x_0^2}{2\tau},$$

with x_0 thickness of a new phase in as-deposited state; x thickness of the new phase after annealing; τ annealing time.

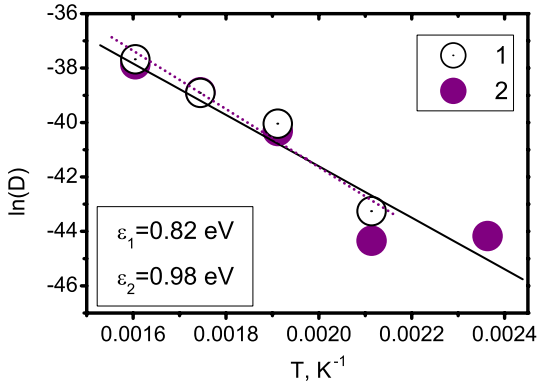

Fig. 6 Arrhenius plots to extract activation energies and pre-exponential factors for the process of diffusional intermixing accompanied by the formation of monosilicide ScSi ($T < 625$ K)

Having no scandium silicide interlayers in the samples with barrier in the initial state, we can omit the term x_0^2. To determine diffusivities for the region where formation of ScSi silicide proceeds, we took first five experimental points in the annealing curves (Fig. 3) and figured out increments of silicide thickness from the Δd values and tabulated densities. The resulting thicknesses were substituted into the foregoing formula for evaluating diffusivities at each temperature. Then these data were used for construction of Arrhenius plots (Fig. 6) to extract pre-exponential factors and activation energies. We came up with the following diffusivities through the barriers for the first stage:

$$D_1 = (8.7 \pm 0.7) \times 10^{-10} \exp\left(-\frac{0.82 \pm 0.11\,\text{eV}}{kT}\right) \text{cm}^2/\text{s},$$

$$D_2 = (2.4 \pm 0.8) \times 10^{-10} \exp\left(-\frac{0.98 \pm 0.12\,\text{eV}}{kT}\right) \text{cm}^2/\text{s}.$$

On average, the activation energy for the reactive diffusion in the course of ScSi silicide formation amounted to $\varepsilon_{\text{BL}} \sim 0.9$ eV.

By applying the same method for the second stage where Sc_3Si_5 silicide is slow in phase formation, we obtained similar parameters for such diffusion process, too:

$$D_{10} = (6.7 \pm 5.8) \times 10^{-8} \exp\left(-\frac{1.34 \pm 0.12\,\text{eV}}{kT}\right) \text{cm}^2/\text{s},$$

$$D_{20} = (3.2 \pm 3.1) \times 10^{-8} \exp\left(-\frac{1.37 \pm 0.30\,\text{eV}}{kT}\right) \text{cm}^2/\text{s}.$$

Activation energy of Sc_3Si_5 formation for both samples averages $\varepsilon_{\text{BH}} \sim 1.36$ eV.

Diffusion characteristics were also determined for Sc/Si MXMs without barriers, where an activation energy of $\varepsilon_{\text{ML}} \sim 0.42$ eV was found for the stage of the monosilicide formation (first three points in Fig. 3), and the following slow transition ScSi $\rightarrow$ Sc_3Si_5 was activated with energy of $\varepsilon_{\text{MH}} \sim 1.23$ eV.

It should be noted that in the sequence of isothermal annealings [33] of Sc/Si MXMs the activation energy for Si atoms diffusing through ScSi layers was found to be $\varepsilon \sim 1$ eV for long annealing times ($\tau > 7$ h) when the diffusion obeys a parabolic law. This value is distinctly higher than 0.42 eV obtained in the present work that may be due to the following circumstances. Annealings for shorter times ($\tau < 4$ h) corresponded to a stage of fast diffusion associated with the presence of excess free volume (or quasivacancies) generated in growing amorphous ScSi silicide [34, 43]. At this stage the activation energy for Si atoms diffusing through growing ScSi interlayers of reduced density was markedly lower than 1 eV. As the diffusion advanced, the fraction of excess free volume diminished and the activation energy raised. Similar results were obtained for Mo/Si MXMs where the activation energy of the interdiffusion was shown to vary several-fold within the first 4 h of the annealing [44]. Barrier layers of CrB_2 are structurally amorphous, may be less dense and may contain an excess free volume. In addition, on interacting with silicon they can form nonstoichiometric amorphous compounds that may also bring about an appearance of excess free volume and respectively a reduction of the activation energy.

As evident from the data of this subsection, the activation energy during ScSi formation is approximately doubled with an insertion of barrier layers. So, it suggests that diffusion of Si atoms through barrier layers is the rate-determining process here. In other words, the application of CrB_2 barrier layers is highly effective as long as ScSi formation is taking place. In the particular case of this study, the working temperatures for Sc/CrB_2/Si MXMs have been extended at least by ~100° (up to $T \sim 475$ K). On the other hand, the resultant average activation energies for the second stage (formation of Sc_3Si_5) are close for MXMs of both types. Therefore, for this stage of phase formation it is a penetration of atomic silicon through Sc_3Si_5 interlayers that is the rate-determining process.

The obtained data allows also making a conclusion that received activation energies for Sc/Si and Sc/CrB_2/Si MXMs based on one-hour annealings are underestimated and are qualitative in character at least for prolonged annealings.

3.4 Comparison of stabilities for Sc/Si MXMs with different barriers

One of the signs for stability of MXM optical performance is the period stability. The period variation produces a shift in the resonance wavelength and at a fixed configuration of the optical scheme terminates in a reflectivity drop faster than may occur due to diffusion intermixing and roughness growth. For instance, a MXM with a CrB_2 barrier layer of nominal thickness (an interaction of barriers with MXM materials is disregarded here), the period of $d_0 \sim 27$ nm and the interface roughness of $\sigma \sim 0.7$ nm has a predicted reflectivity of $R \sim 43\%$ at $\lambda = 47$ nm and normal incidence. The period contraction of $\Delta d \sim 1$ nm caused by ScSi formation (this corresponds to the annealing temperature of ~550 K in Fig. 3) produces the reflectivity drop by ~10% though the reflectivity in the shifted maximum is little affected and is calculated to be ~42% ($\lambda = 45.7$ nm). Meanwhile, the highest possible drop in the reflectivity therewith at the expense of roughness grown up to ~1.8 nm (at temperatures higher 700 K only) comes to just ~6%.

Therefore, it is the period stability that is the proper parameter for the evaluation of MXM resistance. Since a number of publications on Sc/Si MXMs with different barrier materials appeared, we made a comparison of Sc/CrB_2/Si behavior with published ones. Multilayer periods vary widely, so for the validity of such comparison we extracted absolute changes of periods from the published data and then divided them by 27 nm assuming that in the as-deposited state all samples had equal periods. Experimental points resulting from this treatment for Sc/Si MXMs with barrier layers of W [20], ScN [21], B_4C [21] and Cr [22] together with results from the present study are entered in the graph (Fig. 7). Since adjacent barriers are dissimilar in Sc/CrB_2/Si MXMs while barrier layers in other MXMs are the same at both interfaces ($t_{ScN} = t_{B_4C} \sim 0.3$ nm [21]), we took doubled values of period contractions for MXMs with CrB_2 barriers assuming that everywhere over the region of annealing temperatures silicon diffuses through the thin barriers only. Smallest thicknesses of Cr and W barrier layers were 0.7 and 0.8 nm, correspondingly. Although these barriers are noticeably thicker than 0.3 nm, we left them in Fig. 7 for a qualitative comparison. One experimental value for a W/Sc/W/Si MXM with barrier layers ~0.24-nm thick being annealed at ~500 K for 1 h was added, too [45].

The multilayer with Cr barriers, as may be seen from Fig. 7, has a modest stability compared to other MXMs

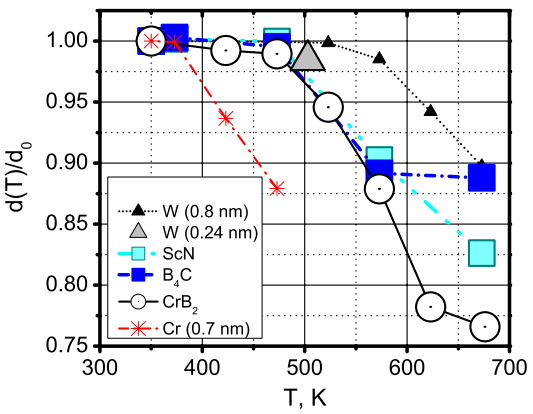

Fig. 7 Comparison of thermal stabilities for Sc/CrB_2/Si MXM and other MXMs taken from different publications. For the validity of the comparison, all period changes were normalized to the equal initial period value of 27 nm

even at rather large barrier thickness (0.7 nm). By resistance, they are ∼200° inferior to MXMs with tungsten barriers of the same thickness and ∼100° to other MXMs with thinner (0.3 nm) barriers. So, these results demonstrate that CrB_2 barriers, as has been expected, are more effective than Cr ones. Multilayers with ScN, B_4C and CrB_2 barriers behave identically up to the annealing temperatures of ∼575 K where period contractions are under ∼10% (<2.7 nm): they are virtually stable (contractions are less than 1%) below ∼475 K and start degrading at higher temperatures. This stage of degradation should correspond to the transition Sc + Si → ScSi (Fig. 3). After 575 K they degrade variously: least contractions have MXMs with B_4C barrier and largest ones are observed in Sc/CrB_2/Si MXMs. Possibly, beginning from 625 K, the thick CrB_2 barrier begins transmitting Si atoms, so the period drift may be overestimated for the studied MXMs. As is established in the present work, at elevated temperatures ($T > 625$ K) the degradation is related to the formation of Sc_3Si_5. A considerable retardation of degradation rate for Sc/B_4C/Si MXM implies that indirectly. Meanwhile, Sc/ScN/Si MXM continues degrading in the same manner. It may be due to a different degree of barrier interaction. As far as could be correct judging from one value, a behavior of MXMs with thin barrier layers of W ($t_W \sim 0.24$ nm) is also close to those for other MXMs with thin barriers. So, with the exception of chromium, all considered barrier materials behave similarly.

4 Discussion

A barrier should prevent diffusion migration of components which may occur through vacancies or interstitials. Activation energy of substitutional diffusion for crystalline matter is directly related to its melting temperature [46], and that of interstitial diffusion depends mostly on atomic density. Therefore, it is preferable to select a barrier material having high melting temperature or atomic density according to a dominant mechanism of diffusion. In the case of an amorphous structure of layers, which is often observed in the thin-film state in the presence of silicon [47–49], a combination of both characteristics is required.

To clarify the reasons for close behavior for different barriers and the particular situation of Cr, we compared their melting temperatures and atomic densities in bulk. Collected data are listed in Table 1. As can be seen, tungsten is the most refractory among the compared materials: its melting temperature is about 1480° higher than that for Cr and ∼740° above the immediately following scandium nitride. Materials of CrB_2 and B_4C are most dense, being appreciably ahead of other considered materials. If the mechanism of the substitutional diffusion is dominant, then the least effective barrier should be chromium and the most effective ones are W and ScN. In the case of the interstitial diffusion the most stable barriers should be CrB_2 and B_4C while the least stable one is tungsten.

Formal application of this approach indicates a tendency toward the interstitial diffusion mechanism as, despite the proximity in the behaviors of different barriers, one can notice a small distinction in MXM stabilities and establish their hierarchy for temperatures of $T < 575$ K (Fig. 7) as W, ScN, B_4C, CrB_2 and Cr that correlates with their melting temperatures (see Table 1). However, the barrier layers may react with MXM material during the fabrication process, which may essentially modify the barrier properties. In this study we observed the interaction of the barrier layers with MXM material (Fig. 2) resulting in their enlargement. Concerning other barriers, it is known [50–52] that amorphous silicide WSi_2 is formed at the interfaces in W/Si MXMs during deposition, and a deposition of chromium on Si brings about the formation of $CrSi_2$ silicide [53]. Data for the melting temperatures and atomic densities of the latter silicides are also added to Table 1 (last two columns). As we can see now, the situation has changed with regard to new data: now WSi_2 has a lower melting temperature compared to all other compounds with the exception of $CrSi_2$.

We tried to seek a regularity in barrier characteristics associated with a possible modification of their composition leaning upon equilibrium phase diagrams of binary alloys, but failed to reveal any correlation between demonstrated stabilities and melting temperatures of possible compounds or atomic densities of the constituent substances. Presumably, the real characteristics of barrier layers, especially thin ones, must be considered (specifically, composition, continuity etc.) that may perceptibly influence barrier penetrability at the nano-scale level.

It is interesting to note that Sc_3Si_5 silicide is the second in the tabulated values of both the melting temperature and the atomic density as compared not only to CrB_2 and any of the possible products of the reaction between CrB_2 and Si but also to ScSi. So, we suppose that a larger fraction of excess free volume (or lower density) in growing ScSi

Table 1 Tabulated data for melting temperatures (T_M) and atomic densities of different barrier materials

Material	W	Cr	B_4C	ScN	CrB_2	WSi_2	$CrSi_2$
T_M (K)	3660	2176	2623	2923	2473	2438	1748
Atomic density (atoms/nm^3)	63.1	83.3	137.1	85.8	137.4	74.2	83.1

relative to Sc_3Si_5 may be one of the reasons for such striking difference in activation energies for the Si-atom diffusion through these silicides. The higher annealing temperatures facilitate a densification of Sc_3Si_5.

So, it is also important to control the excess free volume or the density of barrier layers as the next step of intensive enhancement of such barrier characteristics as a 'sealing ability'. There are described different techniques and procedures which could be useful to density the films, for instance by heating [54], optimizing the energy of depositing atoms (or ions) [35, 55], modifying the layer composition [56] etc. However, taking into account the amorphism and nano-scale dimensions of barrier layers, it is not easy to accomplish such control as the solving of this problem requires an application of special techniques and/or special samples.

5 Conclusions

Thermal stability of Sc/Si multilayer X-ray mirrors with periods of ~27 nm and CrB_2 barrier layers 0.3-nm thick (Sc-on-Si interface) and 0.7-nm thick (Si-on-Sc interface) within the temperature range of 425–780 K was studied. In the as-deposited state all barrier and Si layers have amorphous structure; Sc layers are crystalline. Partial interaction of barrier layers with Si is observed in the as-deposited layers that brings about their enlargement by ~0.6 nm. Nevertheless, they are inert to the matrix materials during annealing up to 625 K keeping the initial thickness.

Silicon atoms are the fast diffusion species controlling the rate of reactive diffusion intermixing of Sc/CrB_2/Si multilayers.

Degradation of Sc/CrB_2/Si MXMs was shown to connect with silicide formation accompanied by period contractions exceeding 5 nm at maximal annealing temperature. It proceeds in a two-stage manner starting with the formation of monosilicide ScSi ($T < 625$ K) and followed by substituting it with silicide Sc_3Si_5 ($T > 625$ K). Both silicides are amorphous and have lower densities compared to bulk.

For the first stage of degradation, it is the diffusion of Si atoms through barrier layers that is the rate-determining process. In this case an introduction of barriers increases the activation energy at least by a factor of two, i.e. the presence of barrier layers is highly efficient here. For the second stage, the diffusion of Si through Sc_3Si_5 is the rate-determining process, i.e. the presence of barriers is almost insensitive. Difference in fractions of excess free volume for these silicides is the cause of this distinction.

The grown fracture of the high-absorbing layer is a subsidiary mechanism of multilayer degradation. Interface roughening is not important.

The resistance of Sc/CrB_2/Si MXMs even with thinner barrier layers was demonstrated to rise at least by 100° in comparison with Sc/Cr/Si ones. It was also demonstrated that with CrB_2 material it is possible to deposit barrier layers of subnanometer thickness, i.e. at least three times as thin as interlayer thickness in Sc/Si MXMs.

For intensively enhancing the resistance of Sc/Si MXMs, it is necessary to control the real characteristics of thin barrier layers, especially their composition and density (excess free volume).

Acknowledgements YPP acknowledges ISKCON for the help in understanding the place and the meaning of this study. This article is based on work supported by the Ukrainian Ministry of Education and Science under contract no. M5473.

Appendix

In the present work we used an empirical formula to estimate the interface roughness (σ) in MXMs deduced from the following simple reasoning. We supposed that for the observation of a diffraction maximum at some angle (θ) in any periodic system it is required for the roughness to be less than a period (d), i.e. $\sigma < d$, otherwise within the single period a specular scattering may occur in antiphase at peaks and valleys. It is known that if we rewrite Bragg's law in the form

$$2\frac{d}{n}\sin\theta_n = \lambda,$$

then an observation of nth order at Bragg angle θ_n is equivalent to an observation of the first order for the MXM with a period of d/n at the same angle. In accordance with the optical theory of reflection by layered periodic systems [57], a reflective maximum occurs as a result of in-phase addition of reflective amplitudes from all interfaces alternating with a step of $t_s \sim d/2$ (continuum theory). Furthermore, the theory of X-ray scattering [58] for layered systems predicts an ultimate reflection as a sum of amplitudes scattered by each layer, and in turn each amplitude is the sum of amplitudes scattered by all atoms in the relevant layer (discontinuum theory). In this case scattering centers are also alternating with the step of $t_s \sim d/2$. Despite different approaches in conceptions with respect to the reflective medium (continuum–discontinuum), both theories give similar results and suggest equal conclusions. In other words, the roughness should be less than the characteristic distance t_s rather than the period of the layered system. To estimate the top value for the roughness, this condition can also be applied as

$$\sigma_{MAX} < \frac{d}{2n}.$$

This formula gives the top roughness estimation in the sense that the layer ratio within the MXM period may bring

about a suppression of the $(n+1)$th maximum in the reflection curve, and we overestimate the roughness in evaluating it by the nth maximum. Besides, the detection of high-order maxima can be limited by an ability of the measuring equipment. In our case the dynamical range ensuring the measurement of the reflection curve was seven orders. According to our experience it is enough to consider the latter condition as not essential. Despite an approximate character, this method may be helpful in the case when, for example, the substrate is not flat or it is bent that brings about a distortion of the reflection curve. Precise knowledge of the period fraction is not necessary here, too.

References

1. http://henke.lbl.gov/cgi-bin/mldata.pl (2011)
2. B. Kjornrattanawanich, D.L. Windt, J.F. Seely, Yu.A. Uspenskii, Appl. Opt. **45**, 1765 (2006)
3. D.L. Windt, J.A. Bellotti, B. Kjornrattanawanich, J.F. Seely, Appl. Opt. **48**, 5502 (2009)
4. J.H. Zhao, M. Zhang, R.P. Liu, X.Y. Zhang, L.M. Cao, D.Y. Dai, H. Chen, Y.F. Xu, W.K. Wang, J. Mater. Res. **14**, 2888 (1999)
5. Y.P. Pershyn, E.N. Zubarev, D.L. Voronov, V.A. Sevryukova, V.V. Kondratenko, G. Vaschenko, M. Grisham, C.S. Menoni, J.J. Rocca, I.A. Artioukov, Y.A. Uspenskii, A.V. Vinogradov, J. Phys. D, Appl. Phys. **42**, 125407 (2009)
6. J. DuMond, J.P. Youtz, J. Appl. Phys. **11**, 357 (1940)
7. P. Yang, U. Klemradt, Y. Tao, J. Peisl, J. Appl. Phys. **86**, 267 (1999)
8. A.I. Fedorenko, S.D. Fanchenko, V.V. Kondratenko, Yu.P. Pershin, A.G. Ponomarenko, E.N. Zubarev, S.A. Yulin, in *4th Int. Conf. Synchrotron Radiation Instrumentation*, Chester, UK, 15–19 July 1991 (1992), p. C7
9. H. Nakajima, H. Fujimori, M. Koiwa, J. Appl. Phys. **63**, 1046 (1988)
10. V.V. Kondratenko, Yu.P. Pershin, O.V. Poltseva, A.I. Fedorenko, E.N. Zubarev, S.A. Yulin, I.V. Kozhevnikov, S.I. Sagitov, V.A. Chirkov, V.E. Levashov, A.V. Vinogradov, Appl. Opt. **32**, 1811 (1993)
11. H. Takenaka, T. Kawamura, J. Electron Spectrosc. Relat. Phenom. **8**, 381 (1996)
12. S. Bajt, J.B. Alameda, T.W. Barbee, W.M. Clift, J.A. Folta, B. Kaufmann, E.A. Spiller, Opt. Eng. **41**, 1797 (2002)
13. Yu.A. Uspenskii, V.E. Levashov, A.V. Vinogradov, A.I. Fedorenko, V.V. Kondratenko, Yu.P. Pershin, E.N. Zubarev, V.Yu. Fedotov, Opt. Lett. **23**, 771 (1998)
14. C.H. Moreno, M.C. Marconi, K. Kanizay, J.J. Rocca, Yu.A. Uspenskii, A.V. Vinogradov, Yu.P. Pershyn, Phys. Rev. E **60**, 911 (1999)
15. B.R. Benware, M. Seminario, A.I. Lecher, J.J. Rocca, Yu.A. Uspenskii, A.V. Vinogradov, V.V. Kondratenko, Yu.P. Pershyn, B. Bach, J. Opt. Soc. Am. B **18**, 1041 (2001)
16. I.A. Artioukov, B.R. Benware, R.M. Fechtchenko, J.J. Rocca, M. Seminario, A.V. Vinogradov, M. Yamamoto, J. Phys. IV Fr. **11**, Pr2-451 (2001)
17. J.F. Seely, Yu.A. Uspenskii, Yu.P. Pershyn, V.V. Kondratenko, V.V. Vinogradov, Appl. Opt. **41**, 1846 (2002)
18. G. Vaschenko, F. Brizuela, C. Brewer, M. Grisham, H. Mancini, C.S. Menoni, M.C. Marconi, J.J. Rocca, W. Chao, J.A. Liddle, E.H. Anderson, D.T. Attwood, A.V. Vinogradov, I.A. Artioukov, Yu.P. Pershyn, V.V. Kondratenko, Opt. Lett. **30**, 2095 (2005)
19. I.A. Artioukov, B.R. Benware, A.V. Vinogradov, Yu.S. Kas'yanov, V.V. Kondratenko, C.D. Macchietto, A. Ozols, J.J. Rocca, J.L.A. Chilla, Quantum Electron. **30**, 328 (2000)
20. D.L. Voronov, E.N. Zubarev, A.V. Penkov, Yu.P. Pershyn, A.G. Ponomarenko, I.A. Artioukov, A.V. Vinogradov, Yu.A. Uspenskii, J.F. Seely, in *Proc. X-ray Lasers 2002: 8th Int. Conf. X-ray Lasers*, Aspen, Colorado, 27–31 May 2002. AIP Conf. Proc., vol. 641 (AIP, Melville, 2002), pp. 575–582
21. J. Gautier, F. Delmotte, M. Roulliay, M.F. Ravet, F. Bridou, A. Jerome, A. Giglia, S. Nannarone, Proc. SPIE **5963**, 59630X.1 (2005)
22. S. Yulin, F. Schafers, T. Feigl, N. Kaiser, Proc. SPIE **5193**, 155 (2003)
23. M. Grisham, G. Vaschenko, C.S. Menoni, J.J. Rocca, Yu.P. Pershyn, E.N. Zubarev, D.L. Voronov, V.A. Sevryukova, V.V. Kondratenko, A.V. Vinogradov, I.A. Artioukov, Opt. Lett. **29**, 620 (2004)
24. A.I. Fedorenko, Yu.P. Pershin, O.V. Poltseva, A.G. Ponomarenko, S.S. Sevryukova, D.L. Voronov, E.N. Zubarev, J. X-Ray Sci. Technol. **9**, 35 (2001)
25. N.P. Lyakishev (ed.), *Constitution Diagrams of Binary Metal Systems* (Mashinostroenie, Moscow, 1996), p. 1024 (in Russian)
26. J. Pellega, G. Sade, J. Appl. Phys. **91**, 6099 (2002)
27. J. Sung, D.M. Goedde, G.S. Girolami, J.R. Abelson, J. Appl. Phys. **91**, 3904 (2002)
28. J.C. Bravman, R. Sinclair, J. Electron. Microsc. Tech. **1**, 53 (1984)
29. S. Yulin, T. Feigl, T. Kuhlmann, N. Kaiser, A.I. Fedorenko, V.V. Kondratenko, O.V. Poltseva, V.A. Sevryukova, A.Yu. Zolotarev, E.N. Zubarev, J. Appl. Phys. **92**, 1216 (2002)
30. S. Braun, H. Mai, M. Moss, R. Scholz, A. Leson, Jpn. J. Appl. Phys. **41**, 4074 (2002)
31. D.L. Voronov, E.N. Zubarev, V.V. Kondratenko, A.V. Penkov, Yu.P. Pershin, Adv. Funct. Mater. **9**, 534 (2002)
32. D.L. Voronov, E.N. Zubarev, V.V. Kondratenko, Yu.P. Pershin, V.A. Sevryukova, Y.A. Bugayev, Thin Solid Films **513**, 152 (2006)
33. D.L. Voronov, E.N. Zubarev, V.V. Kondratenko, Yu.P. Pershin, V.A. Sevryukova, Y.A. Bugayev, Adv. Funct. Mater. **15**, 37 (2008)
34. W. Dörner, H. Mehrer, Phys. Rev. B **44**, 101 (1991)
35. J. Amano, R.P.W. Lawson, J. Vac. Sci. Technol. **14**, 695 (1977)
36. A.F. Ruppert, P.D. Persans, G.J. Hughes, K.S. Liang, B. Abeles, W. Lanford, Phys. Rev. B **44**, 11381 (1991)
37. S.M. Heald, B. Nielsen, J. Appl. Phys. **72**, 4669 (1992)
38. J. Gautier, F. Delmotte, F. Bridou, M.F. Ravet, F. Varniere, M. Roulliay, A. Jerome, I. Vickridge, Appl. Phys. A, Mater. Sci. Process. **88**, 719 (2007)
39. W.-H. Wang, H.Y. Bai, M. Zhang, J.H. Zhao, X.Y. Zhang, W.K. Wang, Phys. Rev. B **59**, 10811 (1999)
40. U. Gösele, K.-N. Tu, J. Appl. Phys. **66**, 2619 (1989)
41. K. Holloway, R. Sinclair, J. Less-Common Met. **140**, 139 (1988)
42. E.N. Zubarev, A.V. Zhurba, V.V. Kondratenko, V.I. Pinegyn, V.A. Sevryukova, S.A. Yulin, T. Feigl, N. Kaiser, Thin Solid Films **515**, 7011 (2007)
43. F. Spaepen, Mater. Sci. Eng. **97**, 403 (1988)
44. A.V. Penkov, D.L. Voronov, A.Yu. Devizenko, A.G. Ponomarenko, E.N. Zubarev, Adv. Funct. Mater. **12**, 1 (2005)
45. D.L. Voronov, Phase transformations in Sc/Si and Sc/W/Si/W multilayer film systems. Ph.D. thesis, V.N. Karazin Kharkov National University, 2002 (in Russian)
46. P.G. Sheumon, *Diffusion in Solids* (Metallurgiya, Moscow, 1966), p. 196 (in Russian)
47. P. Ruterana, P. Houdy, P. Boher, J. Appl. Phys. **68**, 1033 (1990)
48. A. Patelli, V. Rigato, G. Salmaso, N.J.M. Carvalho, J.Th.M. De Hosson, E. Bontempi, L.E. Depero, Surf. Coat. Technol. **201**, 143 (2006)
49. T. Böttger, D.C. Meyer, P. Paufler, S. Braun, M. Moss, H. Mai, E. Beyer, Thin Solid Films **444**, 165 (2003)

50. M.M. Hasan, R.J. Highmore, R.E. Somekh, Vacuum **43**, 55 (1992)
51. D.L. Windt, F.E. Christensen, F.A. Harrison, M. Jimenez-Garate, R. Kalyanaraman, P.H. Mao, J. Appl. Phys. **88**, 460 (2000)
52. E.N. Reshetnyak, S.V. Malykhin, Yu.P. Pershin, A.T. Pugachev, Vopr. At. Nauk. Tehn. (3), 161 (2003) (in Russian)
53. L. Lozzi, M. Passacantando, P. Picozzi, S. Santucci, M. De Crescenzi, Surf. Sci. **251–252**, 579 (1991)
54. D.M. Hausmann, Atomic layer deposition of metal oxide thin films. Ph.D. thesis, Harvard University, Cambridge, MA, 2002
55. J. Amano, R.P.W. Lawson, J. Vac. Sci. Technol. **14**, 690 (1977)
56. J.E. Krzanowski, J. Wormwood, Surf. Coat. Technol. **201**, 2942 (2006)
57. E. Spiller, A.E. Rosenbluth, Opt. Eng. **25**, 954 (1986)
58. B.L. Henke, J.Y. Uejio, H.T. Yamada, R.E. Tackaberry, Opt. Eng. **25**, 937 (1986)